AD-A284 376

NASA ICASE
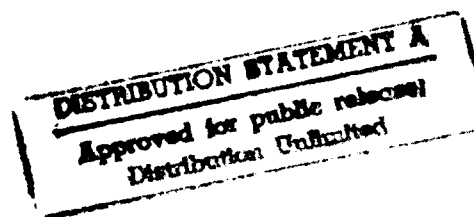
MULTIGRID ONE SHOT METHODS
FOR OPTIMAL CONTROL PROBLEMS:
INFINITE DIMENSIONAL CONTROL

Eyal Arian
Shlomo Ta'asan

94-29783

DTIC
ELECTE
SEP 14 1994
B D

DTIC QUALITY INSPECTED 3

94   079

Multigrid One Shot Methods for Optimal Control Problems: Infinite Dimensional Control

Eyal Arian and Shlomo Ta'asan *
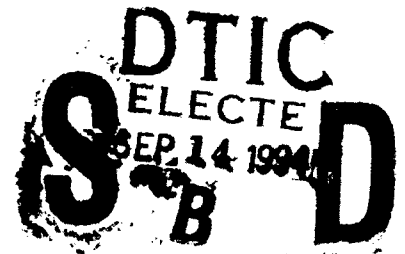The Weizmann Institute of Science, Rehovot. 76100, Israel
Institute for Computer Applications in Science and Engineering
NASA Langley Research Center, Hampton, VA 23681, USA

Abstract

The multigrid one shot method for optimal control problems, governed by elliptic systems, is introduced for the infinite dimensional control space. In this case the control variable is a function whose discrete representation involves increasing number of variables with grid refinement. The minimization algorithm uses Lagrange multipliers to calculate sensitivity gradients. A preconditioned gradient descent algorithm is accelerated by a set of coarse grids. It optimizes for different scales in the representation of the control variable on different discretization levels. An analysis which reduces the problem to the boundary is introduced. It is used to approximate the two level asymptotic convergence rate, to determine the amplitude of the minimization step, and the choice of a high pass filter to be used when necessary. The effectiveness of the method is demonstrated on a series of test problems. The new method enables the solutions of optimal control problems at the same cost of solving the corresponding analysis problems just a few times.

1 Introduction

Numerous computational methods have been developed for predicting the performance of physical systems. For engineering design purposes a modification of the system configuration that results in optimal performance is required. However, computations of large scale optimal control problems are extremely time consuming and in many cases not practical. The effort to overcome such computational difficulties is done in the direction of developing faster computers, on the one hand, and in improving the performance of existing algorithms, on the other hand.

An important and difficult class of optimal control problems are optimal shape design (OSD) of aerodynamic systems [2, 8, 9, 10, 11]; for example, the design of a wing shape. Under certain assumptions, OSD problems can be reduced to simpler optimal boundary control (OBC) problems using the small disturbance approximation [6]. The resulting problems involve a fixed physical domain with control variables that are defined as boundary data. The problem is to minimize a cost function under certain constrains, which are a set of PDEs called "state equations". The cost function is defined to measure the performance of the physical system.

A standard solution process involves an iterative algorithm where each iteration is composed of two steps. First, the control variables are updated with the "sensitivity gradients" which are the gradients of the cost function with respect to the control variables. Then the state variables are updated by solving the constraint equation with the new values of the control variables. The repeated solution of the constraint PDE makes this computation extremely time consuming and in some cases not practical.

Several methods were developed to calculate the sensitivity gradients. Among them is the "adjoint method" [5, 9, 11]. In the adjoint formulation, a Lagrangian is defined together with Lagrange multipliers, which are also called "costate variables". Costate and design equations are derived from the variation of the Lagrangian, and together with the state equation form the necessary conditions for a minimum. The sensitivity gradients are the design equation residuals calculated with the solutions of the state and costate PDEs. The adjoint method was first applied to aerodynamic design by A. Jameson in 1988 [9]. A multigrid (MG) solver was used to accelerate the convergence of the solution of the state and costate equations. This reduces the computational cost of each optimization step to $O(N)$ operations (where N is the number of computational grid points) but does not reduce the number of iterations to reach the minimum.

Originally MG methods were developed to accelerate the convergence rate of the numerical solutions of PDEs [3, 7, 14]. A. Brandt suggested in 1984 [4, page 119] to apply MG methods for optimization problems in the framework of a full multigrid (FMG) algorithm where the optimization problem should be solved on coarse levels and interpolated to finer levels until the finest level is reached. It is further suggested in [4] to treat the optimization problem on all levels where on the finer grids the optimization step should be done locally if possible and the smooth corrections of the error should be done during the coarse grid correction. The whole problem should be solved in one application of the FMG solver.

The adjoint and MG methods were combined to solve an optimal control problem, in "one shot", for the finite dimensional control by S. Ta'asan in 1991 [12]. In the finite dimensional approach, the control variables are represented as a finite sum of some preassigned base functions. The main idea in [12] is to represent the state, the costate and the design equations on coarser grids with the full approximation scheme (FAS)[3]. It is shown in [12] that in general the use of Lagrange multipliers is essential to achieve acceleration of the fine grid solution process by coarser grids. The algorithm optimizes the control variables on coarse grids, and thus, eliminates the repeated solution of fine grid equations in every optimization step. The one shot algorithm was applied successfully to the small disturbance approximation of an aerodynamic wing design problem in a subsonic flow by S. Ta'asan, G. Kuruvila and M. D. Salas (1992) [13]. The performance of the algorithm in [13] was a substantial improvement in terms of computational cost. However, the performance of the finite dimensional one shot algorithm depends on on the choice of base functions and on the level on which the different control variables were optimized.

In this paper we extend the multigrid one shot algorithm to the infinite dimensional control. We introduce an analysis which reduces the problem to the boundary. The analysis is used to to determine a minimization step which reduces mainly the high frequency errors in the control variables. In elliptic systems such a minimization step requires an update of the state and costate solutions only in a local area neighboring the boundary. Based on the above, two level analysis is done to approximate the convergence performance of the algorithm for a given problem and discretization. Computational demonstrations of the algorithm are given for a set of test problems in which the PDE constraint is elliptic.

2 A Single Grid Algorithm for the Solution of Optimal control Problems

2.1 Problem Definition

Let Ω be a bounded open set of $I\!\!R^d$ with smooth boundary Γ and let ϕ be a real valued function on Ω. Let $\mathcal{U}$ and $\mathcal{W}$ be Hilbert spaces of real valued functions which are defined on Γ and Ω respectively.

The problem is to find the "control variable", $u \in \mathcal{U}$, and the "state variable", $\phi \in \mathcal{W}$, such that a given cost function, $F(u, \phi(u))$, defined on $\mathcal{U} \times \mathcal{W}$, will be minimized. Here ϕ satisfies an elliptic PDE which is defined on Ω and will be referred to as the "analysis problem" or the "state equation":

$$\begin{aligned} &\min_{u \in \mathcal{U}} F(u, \phi(u)) && on\ \Gamma \\ &L(\phi, u) = 0 && on\ \Omega \end{aligned} \tag{2.1}$$

Note that the control variable is defined on the boundary Γ, therefore an "optimal boundary control" (OBC) problem is considered.

2.2 Derivation of the Necessary Conditions for a Minimum

We apply the adjoint method to the optimal boundary control problem (2.1). The variable space is enlarged by adding Lagrange multiplier functions or costate variables denoted by λ. A Lagrangian is defined to be the sum of the functional and a linear term in the costate variables which vanishes as the constraint equation is satisfied;

$$E(\phi, \lambda, u) = F(u, \phi) - \langle \lambda, L(\phi, u) \rangle. \tag{2.2}$$

A perturbation of the Lagrangian with respect to all the variables independently, i.e., state, costate and control, results in a variation of the Lagrangian:

$$\begin{aligned} \phi &\leftarrow \phi + \varepsilon \tilde{\phi} \\ \lambda &\leftarrow \lambda + \varepsilon \tilde{\lambda} \\ u &\leftarrow u + \varepsilon \tilde{u} \end{aligned} \tag{2.3}$$

with $\tilde{\phi}, \tilde{\lambda} \in L_2(\Omega)$, $\tilde{u} \in \mathcal{U}$ and ε is a small real parameter. The variation of the Lagrange function, δE, in the first order approximation in ε, is given in the following form:

$$\delta E = -\varepsilon \left\langle \tilde{\phi}, L_\phi^*(\phi, u)\lambda + F_\phi \right\rangle - \varepsilon \left\langle \tilde{\lambda}, L(\phi, u) \right\rangle + \varepsilon \left\langle \tilde{u}, L_u^*(\phi, u)\lambda + F_u \right\rangle \tag{2.4}$$

where L_ϕ^* and L_u^* are the adjoint operators of L_ϕ and L_u respectively. The requirement that the first approximation terms vanish results in the necessary condition for a minimum which will be referred as the state, the costate, and the design equations:

$$\begin{aligned} &\underline{State}: \quad L(\phi, u) = 0 \\ &\underline{Costate}: \quad L_\phi^*(\phi, u)\lambda + F_\phi(\phi, u) = 0 \\ &\underline{control}: \quad L_u^*(\phi, u)\lambda + F_u(\phi, u) = 0. \end{aligned} \tag{2.5}$$

From here on we will use the notation $\mathcal{A}(u)$ for the design equation residual, i.e.,

$$\mathcal{A}(u) = -L_u^*(\phi(u), u)\lambda(u) - F_u(\phi(u), u) \tag{2.6}$$

where $\phi(u)$ and $\lambda(u)$ in (2.6) are solutions of the state and costate equations.

2.3 The Sensitivity Gradients

If the state and costate equations are satisfied, then the variation of the cost function is given by (see Eqn.(2.4)):

$$\delta F = - \langle \tilde{u}, \mathcal{A}(u) \rangle_\Gamma. \tag{2.7}$$

This equation implies that the gradient of the functional with respect to the control variables is given by $-\mathcal{A}(u)$:

$$\nabla_u F(u) = -\mathcal{A}(u). \tag{2.8}$$

Therefore, a perturbation of the control variables with the control residuals multiplied by a small parameter, namely $\tilde{u} = \varepsilon \mathcal{A}(u)$, will result in a reduction of the cost function by

$$\delta F = -\varepsilon \|\mathcal{A}\|_{L_2}^2 + O(\varepsilon^2). \tag{2.9}$$

3

2.4 Discretization

When discretizing the problem it is possible either to derive the necessary conditions for a minimum in the continuous formulation and then discretize or to discretize the functional together with the state equation and then derive the discrete necessary conditions. In the latter case the discrete minimization problem is given by:

$$
\begin{aligned}
&\min_{u^h} F^h(u^h, \phi^h) \qquad &on \ \Gamma^h \\
&L^h(\phi^h, u^h) = 0 \qquad &on \ \Omega^h.
\end{aligned}
\qquad (2.10)
$$

As the grid mesh size, h, goes to zero, solutions of both approaches should converge to the differential solution. However, for finite mesh size discretization and necessary conditions do not necessarily commute. The solutions of both should be within the discretization error from the differential solution. For simplicity in this paper we used the first possibility. The discrete state, costate and design equations are:

$$
\begin{aligned}
&L^h(\phi^h, u^h) = 0 \qquad &on \ \Omega^h \\
&L^{h*}_\phi(\phi^h, u^h)\lambda^h + F^h_\phi(\phi^h, u^h) = 0 \qquad &on \ \Omega^h \\
&L^{h*}_u(\phi^h, u^h)\lambda^h + F^h_u(\phi^h, u^h) = 0 \qquad &on \ \Gamma^h.
\end{aligned}
\qquad (2.11)
$$

We define $A^h(u^h)$ similarly to (2.6).

2.5 A Gradient Descent Algorithm

The following is a gradient descent minimization algorithm which follows immediately from the above.

1. Start with an initial approximation for the control, u_0^h.
2. Solve the state equation for ϕ^h.
3. Solve the costate equation for λ^h.
4. Compute the amplitude of the perturbation, β, with a line search, and update the control variables: $u^h \leftarrow u^h + \beta \ A^h(u^h)$.
5. If the residuals of the state, the costate and the control equations are greater than some preassigned value, in L_2 norm, then goto 2; else stop.

Note that steps 2, 3 and 5 consist of a global computation over the whole domain.

The complexity of this algorithm is given by $O(M^p N^l)$, where M is the number of control parameters, N is the number of grid points, and p and l are integers which depend on the problem and the PDE solver which is used to solve the state and costate equations. For example, if a MG solver is used to solve the PDEs then $l = 1$.

4

3 A Multigrid One Shot Minimization Method

The gradient descent algorithm is applied on a sequence of nested grids, where each coarse grid accelerates the convergence rate of its finer grid. On each grid two processes are employed: relaxation and coarse grid correction of all the variables, including the control variables. On coarse grids the state, the costate and the design equations are restricted from the finer grid with the full approximation scheme [3].

3.1 Relaxation

On each level a relaxation is performed on the state, costate and control variables. The state and costate equations, which are elliptic PDEs, are relaxed by a Gauss-Seidel or damped Jacobi relaxations. The control variables are relaxed by

$$u^h \leftarrow u^h + \beta^h \mathcal{F}^h \mathcal{A}^h(u^h), \tag{3.1}$$

where of β^h and $\mathcal{F}^h$ are chosen to guarantee good smoothing for the control variables, as discussed in Sec.4, and where $\mathcal{A}^h(u^h)$ are the residuals of the design equation. This step should be followed by an update of the state and costate solutions. The construction of β^h and $\mathcal{F}^h$ is done so that the boundary data is updated with a high frequency dominated quantity.

In elliptic systems a perturbation of the boundary condition with a Fourier mode $e^{i\omega x}$ has an exponential decaying effect on the interior solution of the form $e^{-\sigma(\omega)y}$, where y is the distance from the boundary and $\sigma(\omega)$ is a positive monotonically increasing function of ω for large $|\omega|$, [1]. For the Laplace equation the decaying rate is given by $e^{-|\omega|y}$. Therefore, in an MG scheme it is preferable to perturb the boundary condition with only high frequency modes relative to the given level. In that case only local relaxations will be needed in order to update the solutions after each optimization step, resulting in an order $O(N^{\frac{d-1}{d}})$ operations for one optimization step. N is the number of interior grid points on a given level, and d is the space dimension. On the coarsest grid the relaxation of the control variables is given in Sec. 2.5 The PDEs are solved over the whole domain thus taking into account the lowest frequencies. In that way the set of grids is complete in the sense that all Fourier frequencies are treated at some level.

3.2 The Coarse Grid Equations

The restriction of the necessary condition for a minimum to the coarse grid is done with the full approximation scheme (see appendix).

Coarse Grid State Equation

$$
\begin{aligned}
L^H \phi^H &= f_\phi^H \\
f_\phi^H &= I_h^H f_\phi^h + \tau_L^h(\phi^h) \qquad on \ \Omega^H \\
\tau_L^h(\phi^h) &= L^H \tilde{I}_h^H \phi^h - I_h^H L^h \phi^h.
\end{aligned}
\tag{3.2}
$$

where $\tilde{I}_h^H$ and I_h^H are restriction operators which are defined on the interior grid points of the domain Ω^h and which are not necessary identical [3].

Coarse Grid Costate Equation

$$
\begin{aligned}
&L_\phi^{*H}\lambda^H + F_\phi^H = f_\lambda^H \\
&f_\lambda^H = I_h^H f_\lambda^h + \tau_{L_\phi^*}^h(\phi^h, \lambda^h) \\
&\tau_{L_\phi^*}^h(\phi^h, \lambda^h) = L_\phi^{*H} I_h^H \lambda^h + F_\phi^H(I_h^H\phi^h, I_h^H\lambda^h, \bar{I}_h^H u^h) \qquad on\ \Omega^H \qquad (3.3) \\
&\qquad\qquad\qquad - I_h^H\left[L_\phi^{*h}\lambda^h + F_\phi^h(\phi^h, \lambda^h, u^h)\right]
\end{aligned}
$$

Coarse Grid design equation

$$
\begin{aligned}
&L_u^{*H}\lambda^H + F_u^H = f_u^H \\
&f_u^H = I_h^H f_u^h + \tau_{L_u^*}^h(\phi^h, \lambda^h, u^h) \\
&\tau_{L_u^*}^h(\phi^h, \lambda^h, u^h) = L_u^{*H} I_h^H \lambda^h + F_u^H(I_h^H\phi^h, I_h^H\lambda^h, \bar{I}_h^H u^h) \qquad on\ \Gamma^H \qquad (3.4) \\
&\qquad\qquad\qquad - \breve{I}_h^H\left[L_u^{*h}\lambda^h + F_u^h(\phi^h, \lambda^h, u^h)\right]
\end{aligned}
$$

where $\breve{I}_h^H$ and $\bar{I}_h^H$ are restriction operators which are defined on the boundary Γ^h, and where the right hand sides f_ϕ^h, f_λ^h and f_u^h are zero on the finest grid.

3.3 The Coarse Grid Cost Function and Gradient

It can be shown that the full approximation scheme coarse grid equations, (3.2-3.4), are the necessary conditions for a minimum of the following constrained minimization problem:

$$
\begin{aligned}
&\min_{u^H} F^H(u^H, \phi^H) - \langle f_\lambda^H, \phi^H\rangle_W - \langle f_u^H, u^H\rangle_U \qquad on\ \Gamma^H \\
&L^H(\phi^H, u^H) = f_\phi^H \qquad on\ \Omega^H,
\end{aligned}
\qquad (3.5)
$$

where f_ϕ^H, f_λ^H and f_u^H are defined in Eqns.(3.2), (3.3) and (3.4). This implies that the coarse grid gradient is given by

$$
\begin{aligned}
&\nabla_{u^H}^H F^H = \mathcal{A}^H(u^H) \\
&\mathcal{A}^H(u^H) = f_u^H - \left(L_u^{*H}\lambda^H + F_u^H\right).
\end{aligned}
\qquad (3.6)
$$

Thus the relaxation defined by (3.1), on coarse grids, converges to the solution of the coarse grid problem,

$$
\mathcal{A}^H(u^H) = f_u^H - \left(L_u^{*H}\lambda^H + F_u^H\right). \qquad (3.7)
$$

3.4 The One Shot Minimization Algorithm

The problem is solved in one application of an FMG solver. The FMG scheme uses a Vcycle scheme in order to solve the problem on each level. The Vcycle is composed of recursive applications of a relaxation and coarse grid correction. In the following the relaxation, Vcycle and FMG schemes are presented.

Relaxation

A relaxation sweep, $\mathcal{R}^h$, is defined by the following:

1. Perform one relaxation of the state equation for ϕ^h.
2. Perform one relaxation of the costate equation for λ^h.
3. Update the control variables with the design equation residuals,
   $u^h \leftarrow u^h + \beta^h \, \mathcal{F}^h \, \mathcal{A}^h(u^h)$.
4. Perform a few local relaxations of the state and costate
   equations in a narrow strip near the boundary.

Vcycle

The following is a $V^h(\nu_1, \nu_2)$ cycle where ν_1 and ν_2 are integers (in the numerical demonstrations we used $\nu_1 = 2$ and $\nu_2 = 1$). The initial grid is the finest, with a mesh size h.

1. Perform ν_1 relaxation sweeps, $\mathcal{R}^h$.
2. Restrict the state, the costate and the design equations
   to the coarse grid (Eqns.(3.2),(3.3) and (3.4), with $H = 2h$).
   Rescale $h \rightarrow 2h$.
3. If the coarsest level is not reached goto 1.
4. Solve the problem with the standard minimization algorithm
   in Sec. 2.5.
5. Interpolate the coarse grid correction to the finer grid:
   $$\phi^h \leftarrow \phi^h + I_{2h}^h(\phi^{2h} - I_h^{2h}\phi^h) \qquad on \ \Omega^h,$$
   $$\lambda^h \leftarrow \lambda^h + I_{2h}^h(\lambda^{2h} - I_h^{2h}\lambda^h) \qquad on \ \Omega^h,$$
   $$u^h \leftarrow u^h + \bar{I}_{2h}^h(u^{2h} - \bar{I}_h^{2h}u^h) \qquad on \ \Gamma^h.$$
   Rescale $h \rightarrow \frac{h}{2}$.
6. Perform ν_2 relaxation sweeps, $\mathcal{R}^h$.
7. If the finest grid is reached then stop, else goto 5.

FMG cycle

The following is a n-FMG(ν_1, ν_2) cycle to solve the problem with M grids. The coarsest mesh size is denoted by h_c.

1. Start with the coarsest grid, $(h = h_c)$, and solve the problem with
   the standard minimization algorithm in section 2.5.
2. Interpolate the solution to a finer grid, rescale $h \rightarrow \frac{h}{2}$.
3. Perform n times $V^h(\nu_1, \nu_2)$ cycles.
4. if the finest grid is reached then stop, else goto 2.

7

The computational cost of the cycle is $O(N)$ operations, and it reduces the error of the state, costate and control variables by an order of magnitude (in L_2 norm).

4 Fourier Analysis of the Convergence Rate

Fourier analysis of the minimization algorithm is described next. The evolution of high frequency errors, in the control variables, is considered in half space. Then in a standard procedure the problem in half space is reduced to the boundary. A relation between errors and residuals of the design equation, on the boundary, is derived. With this relation the relaxation and coarse grid correction of the control variable are analyzed.

4.1 Reduction to a Boundary Problem

We assume that the state and costate equations are satisfied when the control variables are updated. We are interested in the amplification factor of the error in the control variables as a result of this process. In the vicinity of the boundary, the non-smooth errors can be analyzed using half space geometry. This approximation is valid since in elliptic problems non-smooth Fourier modes decay exponentially into the interior (see Sec. 3.1). Consider a two-dimensional geometry, where the x-axis is parallel to the boundary and the y-axis is in the normal direction. The errors of the state and costate variables satisfy a homogeneous equation in the interior at *every optimization step*, namely

$$\bar{\phi}^h(x,y) = \int_{-\pi}^{\pi} \hat{\phi}^h(\theta, y = 0)e^{ix\cdot\theta/h}e^{-\sigma(\theta)y/h}d\theta$$
$$\bar{\lambda}^h(x,y) = \int_{-\pi}^{\pi} \hat{\lambda}^h(\theta, y = 0)e^{ix\theta/h}e^{-\bar{\sigma}(\theta)y/h}d\theta \qquad (4.1)$$
$$\bar{u}^h(x) = \int_{-\pi}^{\pi} \hat{u}^h(\theta)e^{ix\theta/h}d\theta,$$

where $\sigma(\theta)$ and $\bar{\sigma}(\theta)$ are determined by the interior state equation:

$$L_{\phi}^h e^{ix\theta/h}e^{-\sigma(\theta)y/h} = 0$$
$$L_{\phi}^{h*} e^{ix\theta/h}e^{-\bar{\sigma}(\theta)y/h} = 0. \qquad (4.2)$$

By substituting these expressions into the boundary conditions of the state and costate error equations, we obtain relations between $\hat{\phi}^h(\theta, y = 0), \hat{\lambda}^h(\theta, y = 0)$ and $\hat{u}^h(\theta)$, which are all boundary quantities. Thus, a reduction to a boundary problem has been obtained. From the boundary problem we can deduce a relation between the residuals of the design equation and the errors in the control variables:

$$\hat{\mathcal{A}}^h(\theta) = \hat{T}^h(\theta)\hat{u}^h(\theta). \qquad (4.3)$$

$\hat{T}^h(\theta)$ is the symbol of the Hessian of the cost function, F, subject to the PDE constraint. This symbol determines the smoothing properties of the control variables relaxation as well as the effectiveness of the coarse grid correction, as is discussed next. Note that the explicit form of the operator, T^h, is not known, and in general is a non-local operator. However, the computation of its symbol is straightforward.

8

4.2 The Relaxation

From Eqns.(3.1) and (4.3) it follows that the relation between the errors in the control variables before and after the relaxation is given by

$$\hat{u}^h_{new} = \hat{R}^h(\theta)\hat{u}^h_{old}, \tag{4.4}$$

where the relaxation symbol $\hat{R}^h(\theta)$ is given by

$$\hat{R}^h(\theta) = 1 + \beta^h \hat{\mathcal{F}}^h \hat{T}^h(\theta). \tag{4.5}$$

For multigrid proposes it is desirable for $\hat{R}^h(\theta)$ to have small values in the high-frequency range, ($\frac{\pi}{2} \le |\theta| \le \pi$). In that case the relaxation will reduce effectively the high-frequency errors of the control variables prior to restricting its values to the coarse grid.

Choice of High Pass Filter

In some cases the relaxation without the use of a high pass filter (HPF), $\mathcal{F}^h$, does not smooth the errors effectively for any choice of β^h. In that case an HPF is introduced as a preconditioner of the control residuals. If chosen properly, the symbol $\hat{\mathcal{F}}^h(\theta)\hat{T}^h(\theta)$ is dominated by the high frequencies, and a proper choice of β^h will result in good smoothing. The HPF is particularly effective for problems in which the transformation $\hat{T}^h(\theta)$ is a monotonically decreasing func.ion which has small values in the high frequencies. Without the use of a proper HPF, high-frequency oscillatory errors might enter the control variables during the computation.

Evaluation of the optimization step size β^h

In a multigrid cycle the relaxation should be effective mainly in the high-frequency range. The relaxation parameter β^h is chosen so that the maximum of $|\hat{R}^h(\theta)|$ in the high frequencies will be minimal, that is,

$$\min_{\beta^h} \max_{\frac{\pi}{2} \le |\theta| \le \pi} |1 + \beta^h \hat{\mathcal{F}}^h \hat{T}^h(\theta)|. \tag{4.6}$$

One can show that if the symbol $\hat{T}^h(\theta)$ does not change sign, then β^h is given by

$$\beta^h = -\frac{2}{(\hat{\mathcal{F}}^h\hat{T}^h)_{min} + (\hat{\mathcal{F}}^h\hat{T}^h)_{max}}, \tag{4.7}$$

where $(\hat{\mathcal{F}}^h\hat{T}^h)_{min}$ and $(\hat{\mathcal{F}}^h\hat{T}^h)_{max}$ are the minimal and maximal values of $\hat{\mathcal{F}}^h(\theta)\hat{T}^h(\theta)$ range ($\frac{\pi}{2} \le |\theta| \le \pi$). In most practical problems the symbol $\hat{\mathcal{F}}^h\hat{T}^h(\theta)$ is monotone. Thus β^h is given by

$$\beta^h = -\frac{2}{\hat{\mathcal{F}}^h(\frac{\pi}{2})\hat{T}^h(\frac{\pi}{2}) + \hat{\mathcal{F}}^h(\pi)\hat{T}^h(\pi)}. \tag{4.8}$$

4.3 Two Level Analysis

The process for solving the optimal control problem is equivalent to a process of solving the equation , $T^h e^h = r^h$, where e^h and r^h are the errors and residuals of the design equation,

under the assumption that the state and costate equations are satisfied. Using standard multigrid arguments the two level convergence matrix is given by (See Appendix)

$$M^h(\theta) = R^h(\theta)^{\nu_1} \hat{C}^h(\theta) R^h(\theta)^{\nu_2}, \tag{4.9}$$

where $R^h(\theta)$ is the relaxation matrix

$$R^h(\theta) = \begin{pmatrix} 1 + \beta^h \hat{\mathcal{F}}^h \hat{T}^h(\theta) & 0 \\ 0 & 1 + \beta^h \hat{\mathcal{F}}^h \hat{T}^h(\theta + \pi) \end{pmatrix} \tag{4.10}$$

and $\hat{C}^h(\theta)$ is the coarse grid correction matrix given by

$$\hat{C}^h(\theta) = \begin{pmatrix} 1 & 0 \\ 0 & 1 \end{pmatrix} - \begin{pmatrix} I_H^h(\theta) \\ I_H^h(\theta + \pi) \end{pmatrix} T^H(2\theta)^{-1} \begin{pmatrix} I_h^H(\theta) & , & I_h^H(\theta + \pi) \end{pmatrix} \begin{pmatrix} \hat{T}^h(\theta) & 0 \\ 0 & \hat{T}^h(\theta + \pi) \end{pmatrix}$$

The asymptotic convergence rate is given by the maximum eigenvalue of the matrix $M^h(\theta)$, where θ is in the range $0 < |\theta| \le \pi$.

5 Numerical Examples

In this section we demonstrate the performance of the multigrid one shot algorithm and apply the analysis developed in Sec.4, on a series of test problems. The problems are solved in a two-dimensional domain which is defined by

$$\Omega = \left\{ (x, y) \Big| : 0 \le x \le 1 \; ; \; 0 \le y \le 1 \right\}.$$

The constraint is the Poisson equation and the boundary conditions are periodic in the x-direction and Dirichlet on the lower boundary, $y = 0$. The minimization problem is defined on the upper boundary, $y = 1$.

In subsection 5.1 we solve an optimal control problem of the Dirichlet boundary condition with four different discretizations. The purpose of this example is to study the dependence of the convergence behavior on the choice of discretization. Asymptotic two level convergence rates are estimated with Fourier analysis for the different discretization schemes. The predicted and the actual convergence rates are compared.

In subsection 5.2 we solve an optimal control of the Neumann boundary condition for two different boundary conditions. The purpose of this example is to show the use of the HPF to achieve an efficient smoother for the control variables. The two boundary conditions correspond to qualitatively distinct transformations between error and residuals of the control equation. The two level analysis is used to determine a proper HPF.

5.1 The Dirichlet Boundary Control Problem

Consider the minimization problem is defined by

$$\min_{u(x)} \int_{y=1} \left(\frac{\partial \phi}{\partial n} - f^*(x) \right)^2 dx + \eta \int_{y=1} u^2 dx, \tag{5.1}$$

10

where η is a fixed non negative parameter, $f^*(x)$ is a given function and where ϕ satisfies the state equation

$$\begin{cases} \triangle\phi = f & \text{on } \Omega \\ \phi = u(x) & \text{on } y = 1 \\ \phi = \phi_0 & \text{on } y = 0. \end{cases} \tag{5.2}$$

It is easily verified that the the costate equation is given by

$$\begin{cases} \triangle\lambda = 0 & \text{on } \Omega \\ \lambda + 2(\frac{\partial\phi}{\partial n} - f^*(x)) = 0 & \text{on } y = 1 \\ \lambda = 0 & \text{on } y = 0 \end{cases} \tag{5.3}$$

and the design equation is given by

$$\mathcal{A} = \frac{\partial\lambda}{\partial n} - 2\eta\phi = 0 \quad \text{on } y = 1. \tag{5.4}$$

5.1.1 Discretization

We have used four different discretizations for the minimization problem. For three discretizations all unknowns were defined on the vertices the grid lines (referred to as the "vertex grid"). The control variables are defined on the intersections of the grid with the boundary. In the "cell centered grid" the variables are defined on the centers of the grid cells. The grid is extended out of the domain and virtual cell-centered points are defined on the neighboring exterior of the domain. A Dirichlet boundary condition is given for the average of the variables neighboring the boundary. The control variables are defined on the centers of the segments connecting the intersection of the grid with the boundary. Note that in the multigrid scheme, the vertices of the grids on different scales are nested while in the cell-center case the cells faces are nested.

In the vertex grid we use three different approximations for the normal derivative on the boundary:

1) A first order approximation for the normal derivative

$$V_X 1: \quad \frac{\partial\phi}{\partial n_i} = \frac{\phi_{i,2} - \phi_{i,1}}{h} \tag{5.5}$$

2) A second order approximation for the normal derivative

$$VX2: \quad \frac{\partial\phi}{\partial n_i} = \frac{-\frac{3}{2}\phi_{i,1} + 2\phi_{i,2} - \frac{1}{2}\phi_{i,3}}{h} \tag{5.6}$$

3) A use of a virtual point out of the domain, were its value is determined with the application of the interior operator on the boundary

$$VX3: \quad \frac{\partial\phi}{\partial n_i} = \frac{\phi_{i,1} - \phi_{i,-1}}{2h}. \tag{5.7}$$

A cell centered discretization

$$CC: \quad \frac{\partial\phi}{\partial n_i} = \frac{\phi_{i,\frac{1}{2}} - \phi_{i,-\frac{1}{2}}}{h}. \tag{5.8}$$

11

5.1.2 Reduction to the Boundary

In the following we analyze the design equation of the Dirichlet boundary control problem in the discrete space. We use a second order finite difference approximation of the Laplacian given by

$$\triangle^h = \frac{1}{h^2} \begin{pmatrix} & 1 & \\ 1 & -4 & 1 \\ & 1 & \end{pmatrix}. \tag{5.9}$$

In that case $L_\phi^h = L_\phi^{h*}$ and, therefore, $\sigma(\theta) = \sigma(\theta)$. The term $e^{\sigma(\theta)}$ in Eqn.(4.1) satisfies the following second order equation (see Eqn.(4.2))

$$e^{\sigma(\theta)} + (-4 + 2\cos\theta) + e^{-\sigma(\theta)} = 0. \tag{5.10}$$

The Fourier Symbol of the Normal Derivatives

The normal derivatives, which appear in the design equation, have the following Fourier symbols for the different discretizations:

$$VX1: \quad \frac{\hat{\partial}^h}{\partial n}(\theta) = \frac{e^{-\sigma(\theta)} - 1}{h} \tag{5.11}$$

$$VX2: \quad \frac{\hat{\partial}^h}{\partial n}(\theta) = \frac{-\frac{1}{2}e^{-2\sigma(\theta)} + 2e^{-\sigma(\theta)} - \frac{3}{2}}{h} \tag{5.12}$$

$$VX3: \quad \frac{\hat{\partial}^h}{\partial n}(\theta) = \frac{e^{-\sigma(\theta)} - e^{\sigma(\theta)}}{2h} \tag{5.13}$$

$$CC: \quad \frac{\hat{\partial}^h}{\partial n}(\theta) = \frac{e^{-\frac{1}{2}\sigma(\theta)} - e^{\frac{1}{2}\sigma(\theta)}}{h}. \tag{5.14}$$

The Fourier Symbol of the Design Equation

In terms of the normal derivatives the transformation $\hat{T}^h(\theta)$ (see Eqn.(5.4)) is given by

$$\hat{T}^h(\theta) = -2\left[\left(\frac{\hat{\partial}^h}{\partial n}(\theta)\right)^2 + \eta\right]. \tag{5.15}$$

In this case the calculation of the amplitude of the minimization step, β^h, given by Eqn.(4.8) reduces to

$$\beta^h = \frac{1}{\left(\frac{\hat{\partial}^h}{\partial n}(\frac{\pi}{2})\right)^2 + \left(\frac{\hat{\partial}^h}{\partial n}(\pi)\right)^2 + 2\eta}. \tag{5.16}$$

In Fig.1 the relaxation symbol $\hat{R}^h(\theta) = 1 + \beta^h\hat{T}^h(\theta)$ is plotted for the above four discretizations. For all four discretizations the relaxation reduces the high frequency errors by a factor smaller than 0.5.

Fig.2 depicts the maximal eigenvalue, $|\lambda|_{max}$, of the convergence matrix (4.9) as a function of the number of minimization steps, ν, on a given level. The factor by which the error is reduced as a result of a two level multigrid cycle is bounded by $|\lambda|_{max}$. It is implied by Fig.2 that the cell-centered (CC) and second order vertex (VX2) schemes are expected to have a better performance than the other vertex schemes.
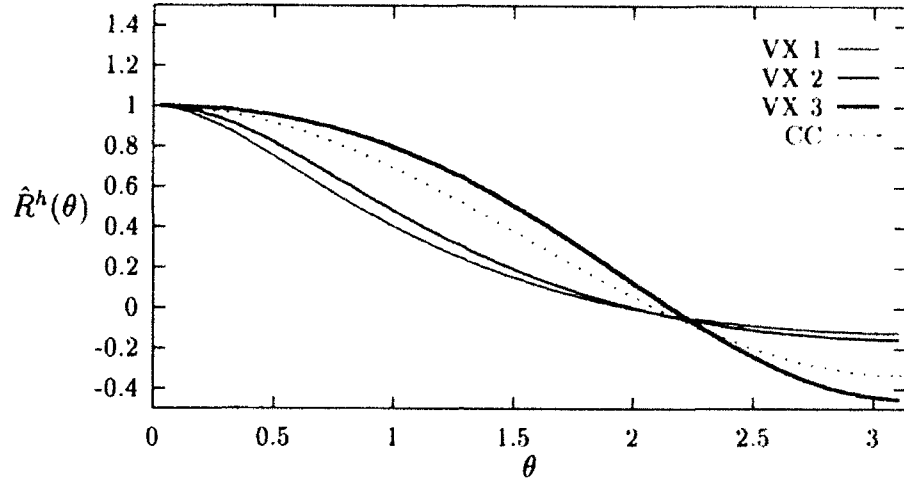
12

Figure 1: The symbol of the control variable relaxation for the Dirichlet boundary control problem with $\eta = 0$.
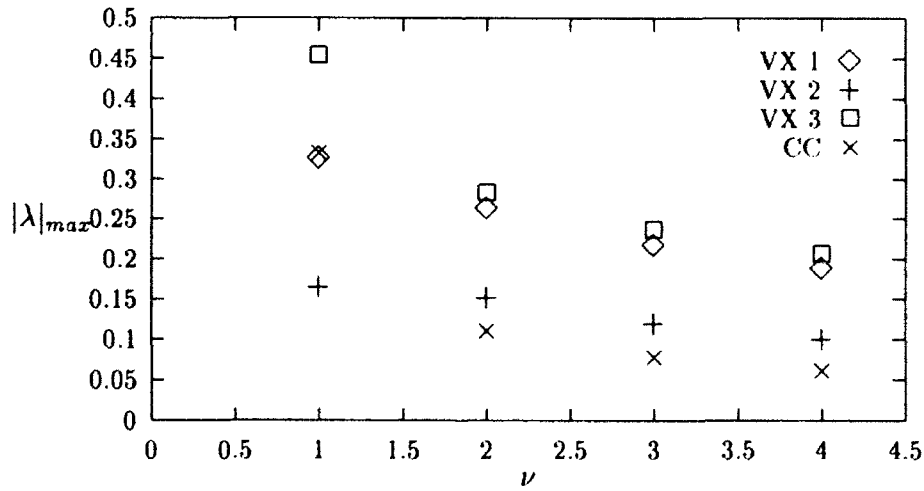

Figure 2: Two level analysis of asymptotic convergence rates, $|\lambda|_{max}$, as a function of the number of optimization steps, ν, for $\eta = 0$.

13

5.1.3 Convergence Performance

In the numerical tests the problem (5.1)-(5.2) was solved for the four discretizations (5.5)-(5.8). In this problem there was no need to use a high pass filter since the transformation $\hat{T}^h(\theta)$ is dominated by the high frequencies in all four discretizations. The minimization step amplitude, β^h, given by Eqn.(5.16) was used in the computations. The multigrid one shot algorithm was tested using between two and seven levels. The two levels convergence is compared with the convergence predicted by the analysis. In all the tests the residuals of the state, the costate and the design equations were computed in L_2 norm.

In the two levels test the finest grid was composed of $2^7 \times 2^7$ grid points and the coarsest grid was composed of $2^6 \times 2^6$ grid points. The parameter η was set to zero. In Fig.3 the two level analysis and the actual convergence rates are compared and the similarity between them is well apparent.

In the multilevel test the fine grid was composed of $2^m \times 2^m$ points, with $m = 5, 6, 7$, and the coarsest grid was composed of 2×2 grid points. The tests with different choices of m were done in order to check if the algorithm is mesh size dependent. All the results in Fig.4 were done with a cell-centered discretization. Since the case $\eta = 0$ in (5.1) corresponds to a trivial problem, the case $\eta = 1$ was tested, although in principle the results should not be different. Fig.4 A shows the convergence performance of the analysis problem (5.3). Figs.4 B and C show the convergence performance of the optimization problem (5.1) with $\eta = 0$ and $\eta = 1$, respectively. The depicted residuals in 4 B and C are the average of the computed state, costate, and design equations residuals.

In all problems the error was reduced in each Vcycle by an order of magnitude, where each Vcycle has a computation complexity of $O(N)$.
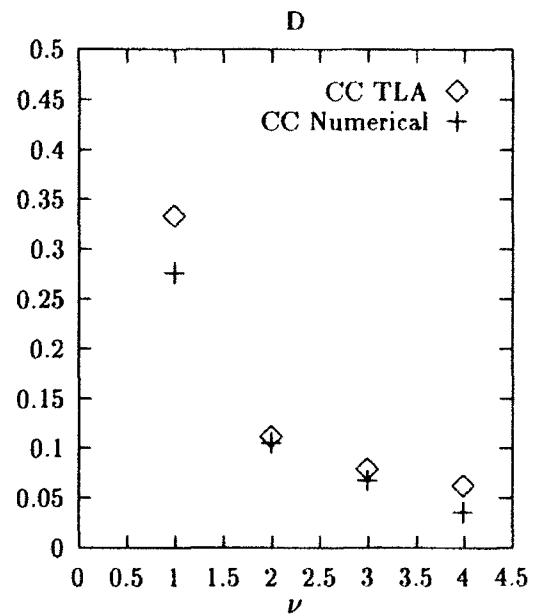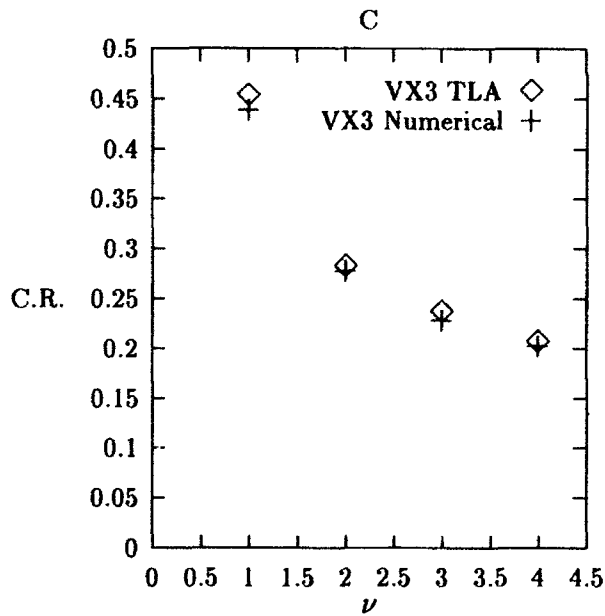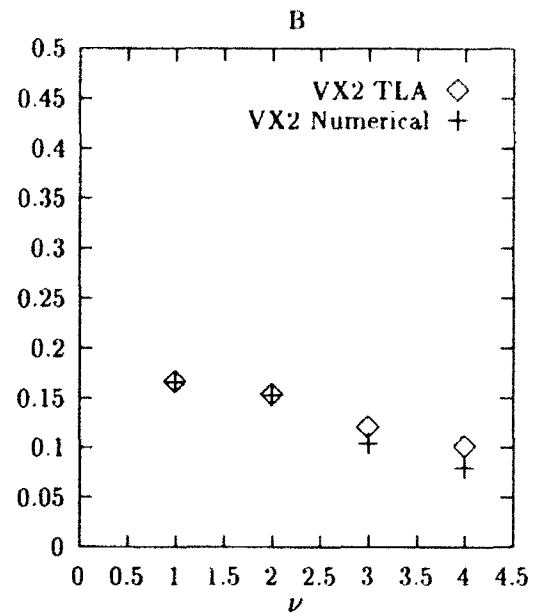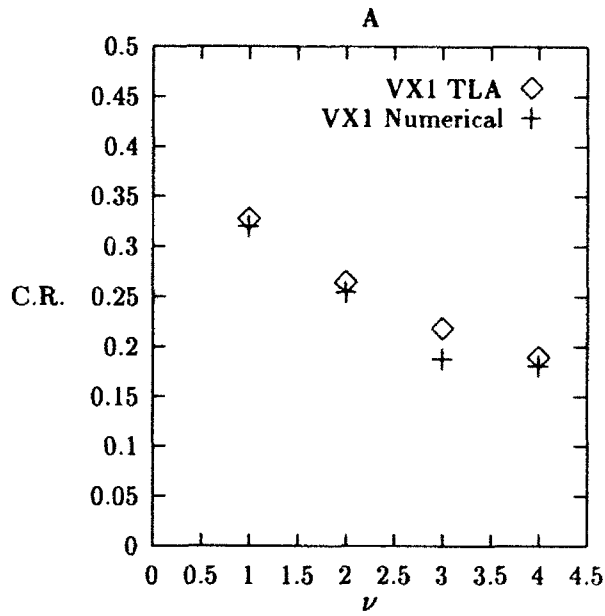
Figure 3: Two level convergence rates (C.R.) of the Dirichlet boundary control problem as a function of minimization steps on the fine level, ν. "TLA" stands for the two level analysis prediction and "Numerical" stands for actual convergence rate. The four figures correspond to different discretization schemes given by (5.11)-(5.14).
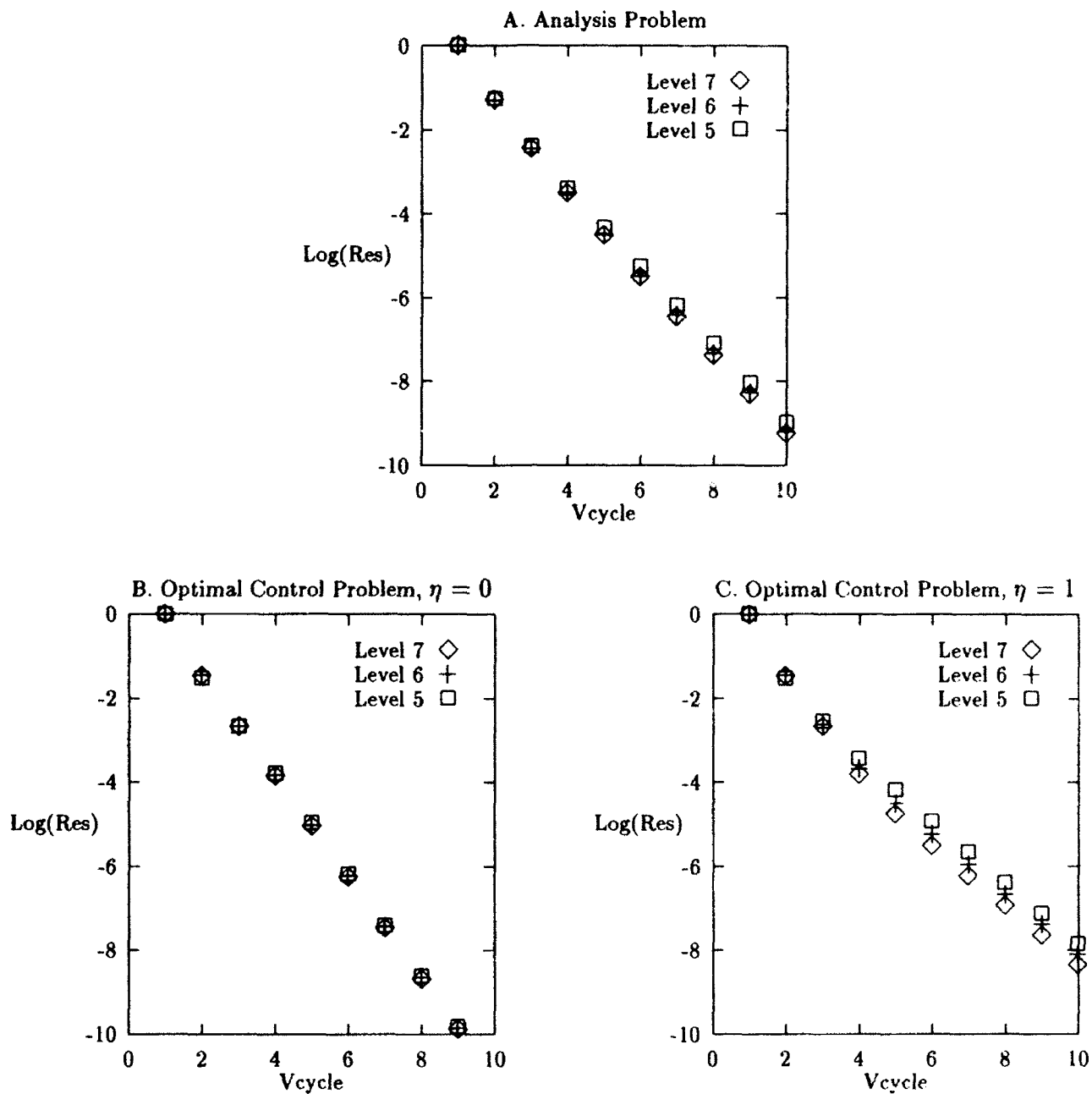
Figure 4: Convergence rates. A. the analysis problem (5.2). B and C the Dirichlet boundary control problem, (5.1)-(5.2), with $\eta = 0$ and $\eta = 1$ respectively.

5.2 The Neumann Boundary Control Problem

In the following examples we compute the Neumann boundary condition on the boundary $y = 1$ such that the values of the solution ϕ on that boundary will match some given function.

The minimization problem is defined by:

$$\min_{u(x)} \int_{y=1} \left(\phi - f^*(x)\right)^2 dx, \tag{5.17}$$

where ϕ is satisfying the state equation

$$\begin{cases} \Delta\phi = f & \text{on } \Omega \\ \frac{\partial\phi}{\partial n} = F(u) & \text{on } y = 1 \\ \phi = \phi_0 & \text{on } y = 0. \end{cases} \tag{5.18}$$

We study the above problem for two different right hand sides of the boundary condition

$$\begin{aligned} F_1(u) &= u \\ F_2(u) &= u_x. \end{aligned} \tag{5.19}$$

It is easily verified that the the costate equation is

$$\begin{cases} \Delta\lambda = 0 & \text{on } \Omega \\ -\frac{\partial\lambda}{\partial n} + 2(\phi - f^*(x)) = 0 & \text{on } y = 1 \\ \lambda = 0 & \text{on } y = 0. \end{cases} \tag{5.20}$$

The design equation is given on the boundary $y = 1$ for the two right hand sides, in the corresponding order, by

$$\begin{aligned} \mathcal{A}_1 &= -\lambda = 0 \\ \mathcal{A}_2 &= \lambda_x = 0. \end{aligned} \tag{5.21}$$

Discretization The state and costate variables were discretized on a cell centered grid. The control variables are defined on the centers of the segments connecting the intersection of the grid with the boundary for the first case: $F_1(u) = u$. In the second case, $F_2(u) = u_x$, the control variables are defined on the intersections of the grid lines with the boundary.

5.2.1 Analysis

The symbols of the transformations $\hat{T}^h(\theta)$ in (4.5) and the proper amplitudes, β^h, calculated with Eqn.(4.8) for the different boundary conditions in (5.19) are given by

$$\begin{aligned} \hat{T}_1^h(\theta) &= -\frac{h^2}{2}\frac{\sqrt{6-2\cos(\theta)}}{1-\cos\theta} \quad ; \quad \beta_1 = \frac{4}{h^2(\sqrt{6}+\sqrt{2})} \\ \hat{T}_2^h(\theta) &= -\sqrt{6-2\cos\theta} \quad ; \quad \beta_2 = \frac{2}{\sqrt{6}+\sqrt{8}} \end{aligned} \tag{5.22}$$

17

One can immediately observe that in the first problem the transformation symbol, $\hat{T}_1^h(\theta)$, is not dominated by the high-frequencies. This means that no choice of β^h can result in a relaxation with good smoothing properties, since high-frequency errors will have a low weight in the residuals of the design equation. For example, $\hat{T}_1^h(\pi) = -\frac{h^2}{\sqrt{2}}$ approaches zero with grid refinement; therefore one should expect very slow convergence for high-frequency errors. For this case the two level analysis predicts a non-converging scheme, i.e., the maximal eigenvalue, $|\lambda|_{max}$, of the convergence matrix (4.9) is greater than one.

In the second problem there is a high-frequency dominance in the symbol $\hat{T}_2^h(\theta)$. Therefore one could expect that a few local relaxations near the boundary are needed after each perturbation of the control variables. In this case the two level analysis predicts the same convergence rate as in the analysis problem, see Fig.6B.

5.2.2 Use of a High Pass Filter

In the first test problem, where $F_1(u) = u$, we can perturb the boundary data with, $D_{xx}\mathcal{A}$, instead of $\mathcal{A}$, where D_{xx} is a second order tangential derivative. In this case the symbol of the design equation will become

$$\hat{D}_{xx}(\theta)\hat{T}_1^h(\theta) = \sqrt{6 - 2\cos(\theta)}, \tag{5.23}$$

resulting in a high frequency dominant symbol. The relaxation parameter changes and is given by

$$\beta_1^h(D_{xx}) = -\frac{2}{\sqrt{6} + \sqrt{8}}. \tag{5.24}$$

A use of a higher order operator such as a fourth order tangential derivative, $\mathcal{F} = D_{xxxx}$, results in

$$\hat{D}_{xxxx}(\theta)\hat{T}_1^h(\theta) = -\frac{2}{h^2}\sqrt{6 - 2\cos(\theta)}(1 - \cos(\theta)) \tag{5.25}$$

with

$$\beta_1^h(D_{xxxx}) = \frac{h^2}{\sqrt{6} + 2\sqrt{8}}. \tag{5.26}$$

The two level analysis gives a much better convergence performance for the first choice, see Fig.6A.

5.2.3 Convergence Performance

The convergence performance of the Neumann boundary control problem is tested for the two cases of boundary condition.

In Fig.7A, the convergence of the optimal control problem (5.17)-(5.18), with $F(u) = u$, is depicted. It is clear from Fig.7A that when using a HPF of the form $\mathcal{F} = D_{xx}$ the converegnce rate is better than that achieved when using $\mathcal{F} = D_{xxxx}$, as predicted by the analysis (Fig.6A). Without using a HPF, ($\mathcal{F} = I$), the algorithm didn't converge and high-frequency oscillatory errors were observed to dominate the solution.
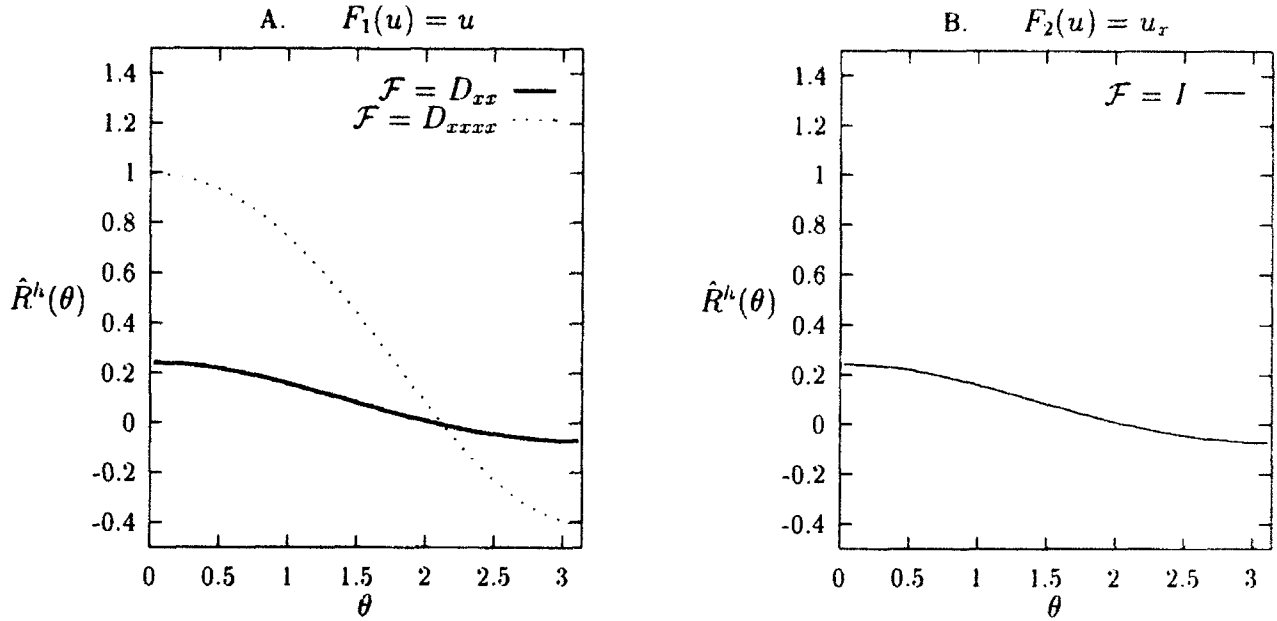
18

Figure 5: The symbol of the control variables relaxation, for the Neumann boundary control problem (5.17)-(5.18). In Fig.A. two different HPF are used, ((5.23) and (5.25)), with their appropriate relaxation parameter β^h, (5.24) and (5.26).

The two level analysis predicts that if the boundary condition is changed to $F(u) = u_x$ in Eqn.(5.18) than no HPF is needed for the problem to converge. Fig.7B shows that this is indeed the case.

6   Conclusion

We have developed a multigrid one shot algorithm to solve the infinite dimensional optimal control problem. An analysis, which is based on the reduction of the problem to the boundary, was performed both to predict the convergence rate of a two grid algorithm and to determine the minimization step. Thus, an expensive line search on every minimization step was not required on fine levels. Numerical demonstrations on a series of two dimensional test problems were performed. In each test problem the amplitude of the the minimization step on fine levels, β^h, and a proper high pass filter (HPF), $\mathcal{F}^h$, was determined using the analysis. Comparison of the two level convergence rates and two level analysis shows agreement within a reasonable error. We find this analysis a simple and powerful tool. In each problem, the minimum was reached at a cost of solving the analysis problem just a few times, independent of grid size.
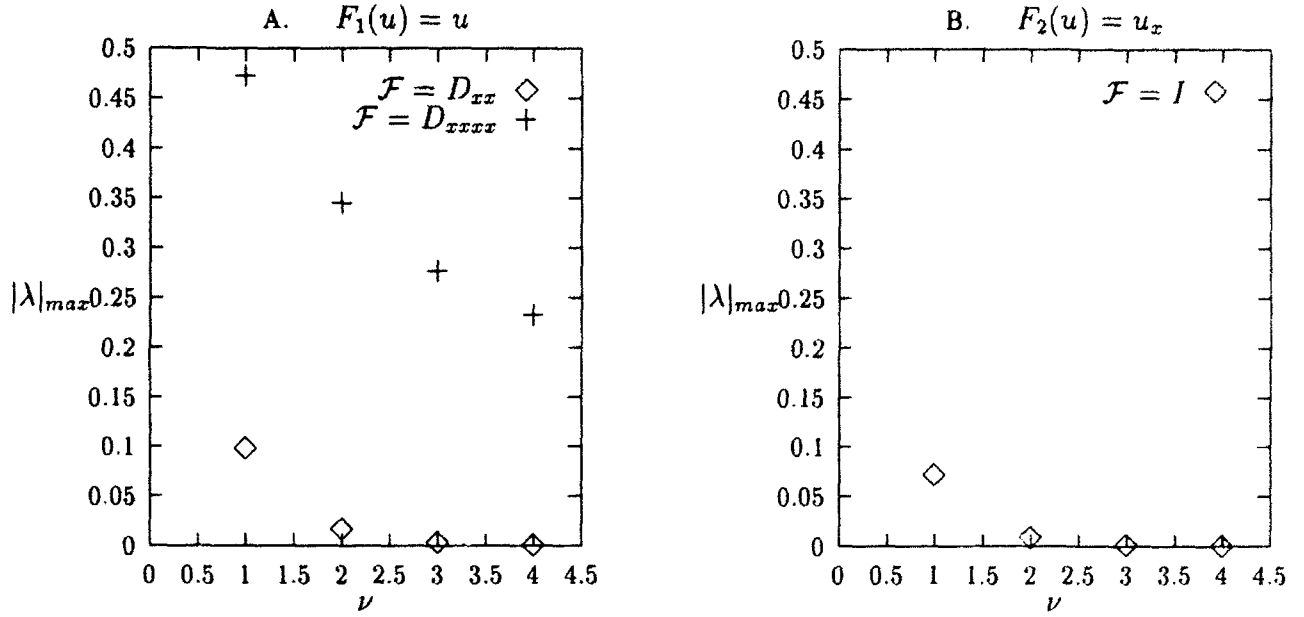
19

Figure 6: Two level analysis convergence rates for two choices of boundary conditions in the Neumann boundary control problem (see Eqn.(5.19)). $\mathcal{F}$ stands for the choice of high pass filter.
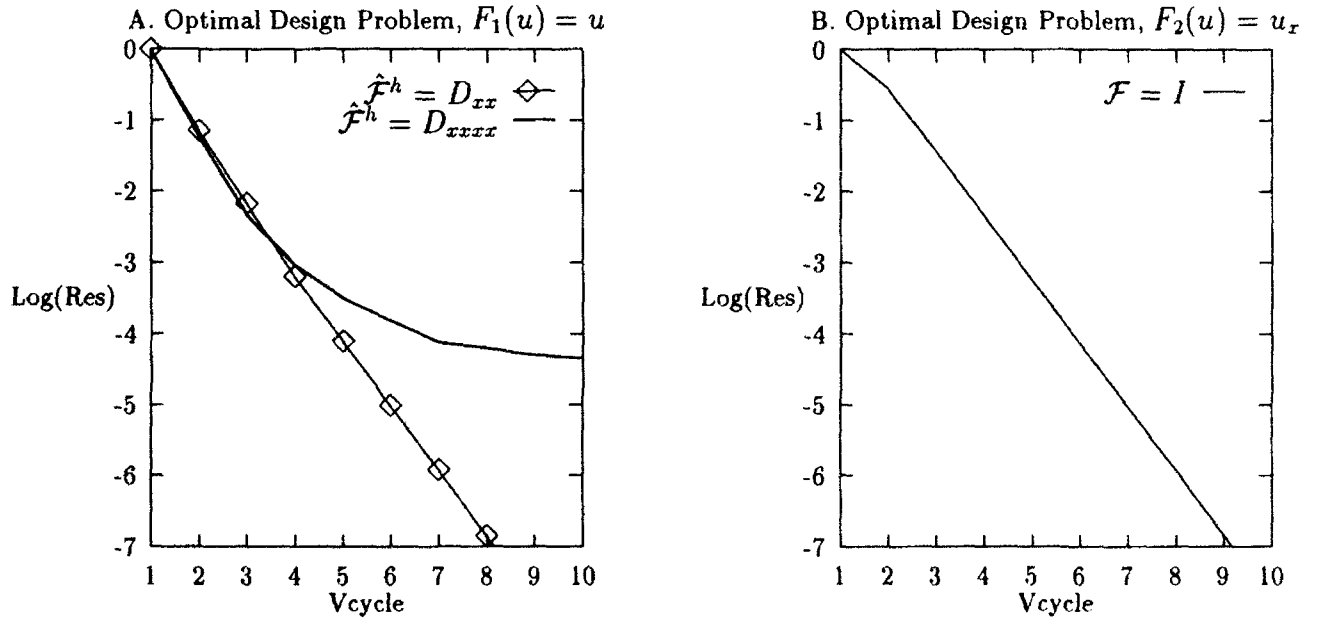

Figure 7: A. Convergence rates for $V(2,1)$ multigrid cycle of the Neumann boundary control problem, with two different HPFs: D_{xx} and D_{xxxx}. Fig. B. No use of HPF is made. Fine grid contains $2^7 \times 2^7$ and coarsest 4 grid points.

A A Short Review of Multigrid Methods for Solving PDEs

The main idea of multigrid is to solve the problem on a set of nested grids. On each grid there are two processes: relaxation and coarse grid correction (CGC). The relaxation smooths the errors while the CGC eliminates effectively the smooth errors. In that way a very efficient algorithm is achieved which reaches the discretization error in $O(N)$ operations, where N is the number of interior grid points. In the following we refer to the solution of a discrete elliptic PDE given by

$$L^h \phi^h = f^h, \tag{A.1}$$

where h is the mesh size.

Coarse Grid Problem

For non-linear problems the coarse grid equations are approximated by the full approximation scheme (FAS):

$$L^H \phi^H = I_h^H f^h + \tau_L^h(\phi^h), \tag{A.2}$$

where I_h^H and I_H^h denote the restriction and interpolation operators, respectively, and where τ_L^h is defined by

$$\tau_L^h(\phi^h) = L^H \bar{I}_h^H \phi^h - I_h^H L^h \phi^h, \tag{A.3}$$

where $\bar{I}_h^H$ and I_h^H are not necessary the same [3]. The coarse grid correction (CGC) is given by

$$\phi_{new}^h = \phi_{old}^h + I_H^h(\phi^H - I_h^H \phi_{old}^h). \tag{A.4}$$

Smoothing Properties

In the infinite space mode analysis the Fourier symbol of the differential operator, L^h, is denoted by $\hat{L}^h(\theta)$. For standard MG to work properly one must have h-elliptic discretization, i.e.

$$|\hat{L}^h(\theta)| \geq C \left| \frac{\theta}{h} \right|^m \qquad for \ \|\theta\| \leq \pi \tag{A.5}$$

where $\hat{L}^h(\theta)$ is the Fourier symbol of L^h and where C is a constant. The consequence of the condition in (A.5) is that the relaxation will be effective mainly for the high frequency errors. For the Jacobi relaxation, the relaxation operator, R^h, is related to the difference operator, L^h, by

$$R^h = I - \beta L^h, \tag{A.6}$$

where I is the identity operator and β is a parameter. The smoothing rate of the relaxation is determined by

$$\max_{\frac{\pi}{2} \leq |\theta| \leq \pi} |R^h(\theta)| \leq C_0 \leq 1, \tag{A.7}$$

where the constant C_0 is the predicted smoothing factor (typical value is 0.5).

Two Level Analysis

For the linear case a two level mode analysis can be done to predict the convergence rate of the multigrid cycle. The full cycle symbol is give by

$$\hat{M}(\theta) = \hat{R}^h(\theta)^{\nu_2}[I - \hat{I}_H^h(\theta)\hat{L}^H(2\theta)^{-1}\hat{I}_h^H(\theta)\hat{L}^h(\theta)]\hat{R}^h(\theta)^{\nu_1}, \tag{A.8}$$

where $\hat{R}^h$ stands for the relaxation operator, I is the unit matrix, $\hat{L}^H$ stands for the coarse grid operator, and ν_1 and ν_2 are integers.

The convergence rate of the cycle is give by

$$\mu = \sup_{0 < |\theta| \leq \frac{\pi}{2}} \|\hat{M}(\theta)\|. \tag{A.9}$$

REFERENCES

[1] Agmon, A. Douglis, L. Nirenberg. Estimates Near the Boundary for Solutions of Elliptic Partial Differential Equations Satisfying General Boundary Conditions. Communications on Pure and Applied Math., Vol. XII 623-727 (1959).

[2] E. Arian, and S. Ta'asan, Shape Optimization in One Shot, Proceedings of a Workshop on Optimal Design and Control held at Blacksburg, VA, April 8-9, 1994.

[3] A. Brandt: Multilevel Adaptive Solutions to Boundary Value Problems, Math. Comp. 31, pp 333-390 (1977).

[4] A. Brandt: Multigrid Techniques: 1984 Guide, with Applications to Fluid Dynamics. GMD Studien 85 from GMD-AIW, Postfach 1240 D-5205, St. Augustine, Germany.

[5] R. Fletcher, Practical Methods of Optimization, *John Wiley & Sons* (1981).

[6] C. Hirsch, Numerical Computation of Internal and External Flows, Vol.2, *John Wiley & Sons* (1988).

[7] W. Hackbusch Multi-Grid Methods and Applications, Springer-Verlag Berlin, Heidelberg (1985).

[8] J. Haslinger and P. Neittaanmäki, Finite Element Approximation for OSD: Theory and Application, *John Wiley & Sons* (1988).

[9] A. Jameson, Aerodynamic Design Via Control Theory, ICASE Report No. 88-64, November (1988), Journal of Scientific Computing. 3:233-260 (1988)

[10] S. Ta'asan, G. Kuruvila, M. D. Salas, Airfoil Optimization by the One-Shot Method, Optimum Design Methods in Aerodynamics, AGARD-FDP-VKI Special Course, April 25-29, (1994)

[11] O. Pironneau, Optimal Shape Design for Elliptic Systems, *Springer Series in Computational Physics* (1983).

[12] S. Ta'asan, "One Shot" Methods for Optimal Control of Distributed Parameter Systems I: Finite Dimensional control, ICASE report NO. 91-2, January (1991).

[13] S. Ta'asan, G. Kuruvila, M. D. Salas, Aerodynamic Design and Optimization in One Shot, 30th Aerospace Sciences Meeting & Exhibit, AIAA 92-0025, Jan. (1992).

[14] P. Wesseling, An Introduction to Multigrid Methods, *John Wiley & Sons* (1991).

REPORT DOCUMENTATION PAGE

1. AGENCY USE ONLY *(Leave blank)*	2. REPORT DATE July 1994	3. REPORT TYPE AND DATES COVERED Contractor Report

4. TITLE AND SUBTITLE
MULTIGRID ONE SHOT METHODS FOR OPTIMAL CONTROL
PROBLEMS: INFINITE DIMENSIONAL CONTROL

5. FUNDING NUMBERS
C NAS1-19480
WU 505-90-52-01

6. AUTHOR(S)
Eyal Arian
Shlomo Ta'asan

7. PERFORMING ORGANIZATION NAME(S) AND ADDRESS(ES)
Institute for Computer Applications in Science
and Engineering
Mail Stop 132C, NASA Langley Research Center
Hampton, VA 23681-0001

8. PERFORMING ORGANIZATION REPORT NUMBER
ICASE Report No. 94-52

9. SPONSORING/MONITORING AGENCY NAME(S) AND ADDRESS(ES)
National Aeronautics and Space Administration
Langley Research Center
Hampton, VA 23681-0001

10. SPONSORING/MONITORING AGENCY REPORT NUMBER
NASA CR-194939
ICASE Report No. 94-52

11. SUPPLEMENTARY NOTES
Langley Technical Monitor: Michael F. Card
Final Report
Submitted to Journal of Computational Physics

12a. DISTRIBUTION/AVAILABILITY STATEMENT
Unclassified-Unlimited
Subject Category 64

12b. DISTRIBUTION CODE

13. ABSTRACT *(Maximum 200 words)*

The multigrid one shot method for optimal control problems, governed by elliptic systems, is introduced for the infinite dimensional control space. In this case the control variable is a function whose discrete representation involves increasing number of variables with grid refinement. The minimization algorithm uses Lagrange multipliers to calculate sensitivity gradients. A preconditioned gradient descent algorithm is accelerated by a set of coarse grids. It optimizes for different scales in the representation of the control variable on different discretization levels. An analysis which reduces the problem to the boundary is introduced. It is used to approximate the two level asymptotic convergence rate, to determine the amplitude of the minimization step, and the choice of a high pass filter to be used when necessary. The effectiveness of the method is demonstrated on a series of test problems. The new method enables the solutions of optimal control problems at the same cost of solving the corresponding analysis problems just a few times.

14. SUBJECT TERMS
optimal control, optimal shape design, multigrid, one-shot, adjoint

15. NUMBER OF PAGES
25

16. PRICE CODE
A03

17. SECURITY CLASSIFICATION OF REPORT Unclassified	18. SECURITY CLASSIFICATION OF THIS PAGE Unclassified	19. SECURITY CLASSIFICATION OF ABSTRACT	20. LIMITATION OF ABSTRACT